

Optimal Design for Three-loop Autopilot Using Multi-Constraint Optimization

Mohamed A. Abd-Elatif* and Qian Longjun

School of Automation, University of Science and Technology, Nanjing 210094, China

Email: Mdyosf2010@Yahoo.com, qlongjun@mail.njust.edu.cn

Abstract—One challenging control problem is that of modern tactical missile systems in pursuit of achieving large scale of maneuverability and sufficient stability. The optimal autopilot for practical systems should provide the fastest possible performance under constraints on applicable system dynamics. The quadratic performance index with weightings adjustment cannot easily and clearly handle such constraints. This paper introduces an optimal autopilot design technique based on the constrained optimization. The tracking performance is formed analytically as the design objective. The open-loop crossover frequency and the maximum demand of the actuator fin-deflection rate are introduced as analytical inequality constraints. The design process is handled into the space of stable poles parameters of the autopilot closed loop characteristic. The introduced autopilot design is self-consistent technique and is easily fulfilled with an optimization algorithm. Numerical simulation results are illustrated to demonstrate the effectiveness and feasibility of the proposed approach.

Index Terms—three loop autopilot, optimal gain design, crossover frequency constraint, control effort constraint

I. INTRODUCTION

The demand for highly maneuverable missile systems is considerably growing which makes the problem of missile autopilot design is a challenging one. The practical missile autopilot must be designed with a guaranteed performance in concert with robustness requirements. These requirements are mainly on the open-loop frequency response and the actuator limits. For instant, Ref. [1,2] shows that ignoring the open-loop crossover frequency value in the design procedure, even with good phase and gain margins, will led to design instability due to an expected modeling perturbation. Reference [3] concludes the reason for such instability is that the model non-linearity is considerably increased which leads to considerable difference between the predicted gain and phase values and their real values at high frequencies. In order to address this problem the crossover frequency value should modified to make sure that the open-loop gain is below some desired level at high frequencies. This value is set based on assumptions about the high-frequency modeling errors, sometimes based on test data, and often comes from hard-learned experience. A classical “rule of thumb” addresses this

value [1,4]. Equally important, the physical limits of the control surface actuators should be considered; otherwise, the performance of the closed-loop system may be significantly degraded or may even become unstable [5].

Basically, classical design approach achieves the desired performance and provides a sufficient stability and robustness [4,6]. This method could be consider as a closed-loop pole assignment technique where the desired poles in the closed-loop characteristic are adjusted to satisfy the design performance in both time and frequency domains. However, this technique is valid for a limited set of flight conditions and system size. Besides, the classical design approach does not guarantee an ideal autopilot as it mostly depends upon the designer manual tuning. On the other hand, LQR is widely recognized as a main design tool in modern control theory. The idea of combined the optimal with classical design aspects shall provide a system that satisfies design constraints requirements and at the same time minimize a performance criterion. For example, optimal autopilot design is introduced based on weightings adjustment for a minimum error between desired and the actual open loop crossover frequency [7-9]. However, this method relies on initial guessing of the weights which might need to be carried out and repeated to adjust the required initial performance. Moreover, this scheme will not essentially guarantee an optimal autopilot as it is possible to get the same crossover frequency for different gain designs. For more realistic applications, the actuator fin deflection rate and the crossover frequency value are considered through a pole adjusting approach in Refs. [10]. Despite its contribution, this approach is yet based on approximate formulas. Besides, it is not offers an optimal solution.

This paper involves in the formulation of an optimal approach that achieves the optimal performance of the autopilot closed-loop characteristic within constraints on the open-loop frequency response and the actuator limits. The design accomplishes for the optimal tracking performance using constrained optimization technique. This paper is organized as follows. Section 2 discusses the three-loop autopilot model of pseudo angle of attack and derives analytical formula between autopilot gains and the design parameters of the stable closed-loop characteristic. Section 3 highlights the open-loop crossover frequency and the actuator fin-deflection rate constraints in the form of inequality functions. In Section 4, the optimal autopilot gain design is achieved using a

Manuscript received January 11, 2017; revised August 1, 2017.

constrained optimization algorithm, where the integral square error (ISE) performance index of the autopilot tracking error is formed analytically as the design objective [11,12]. The whole optimization for both the objective and the constraints are manipulated in terms of the stable characteristic design parameters. Finally, Section 5 shows a numerical autopilot design of a typical missile system using the proposed technique.

II. AUTOPILOT CONFIGURATION AND GAIN FORMULA

Different three-loop topologies are implemented for different autopilot designs. In engineering practice, since the angle of attack (AOA) cannot be directly measured so the approximate AOA is obtained from the angular rate. The autopilot topology, Fig.1, is called pseudo AOA autopilot. The autopilot gain $K = [K_1 \ K_2 \ K_3]$, should be chosen properly to satisfy the desired performance. The under laying missile system is assumed to be symmetrical airframe and roll stabilized where its motion is restricted to the vertical plane. The linearized transfer functions of the missile airframe with ideal actuator and IMU are given as

$$\begin{aligned} G_{\delta}^{a_y}(s) &= \frac{a_y(s)}{\delta(s)} = \frac{K_{q1}(1+T_1s+T_2s^2)}{1 + \frac{2\zeta_{AF}s}{\omega_{AF}} + \frac{s^2}{\omega_{AF}^2}} \\ G_{\delta}^{\dot{\theta}}(s) &= \frac{\dot{\theta}(s)}{\delta(s)} = \frac{K_{q3}(1+T_\alpha s)}{1 + \frac{2\zeta_{AF}s}{\omega_{AF}} + \frac{s^2}{\omega_{AF}^2}} \\ G_{\delta}^{\alpha}(s) &= \frac{\alpha(s)}{\delta(s)} = \frac{K_\alpha K_{q3}(1+B_1s)}{1 + \frac{2\zeta_{AF}s}{\omega_{AF}} + \frac{s^2}{\omega_{AF}^2}} \\ G_{\delta}^{\dot{\alpha}}(s) &= \frac{\dot{\alpha}(s)}{\delta(s)} = K_\alpha \frac{(1+B_1s)}{(1+T_\alpha s)} \end{aligned} \quad (1)$$

where

$$\begin{aligned} \omega_{AF}^2 &= -M_\alpha + Z_\alpha M_q, \quad \zeta_{AF} = \frac{-(Z_\alpha + M_q)}{2\omega_{AF}}, \quad B_1 = \frac{Z_\delta}{M_\delta - Z_\delta M_q}, \\ K_{q1} &= \frac{-V(M_\alpha Z_\delta - M_\delta Z_\alpha)}{M_\alpha - Z_\alpha M_q}, \quad K_{q3} = \frac{K_{q1}}{V}, \quad K_\alpha = \frac{M_\delta - Z_\delta M_q}{M_\alpha Z_\delta - M_\delta Z_\alpha}, \\ T_1 &= \frac{Z_\delta M_q}{M_\alpha Z_\delta - M_\delta Z_\alpha}, \quad T_2 = \frac{Z_\delta}{M_\alpha Z_\delta - M_\delta Z_\alpha}, \quad T_\alpha = \frac{M_\delta}{M_\alpha Z_\delta - M_\delta Z_\alpha}, \end{aligned}$$

ϑ is the body pitch angle, θ is the trajectory angle, α is the AOA, V is the missile velocity, δ is the fin-deflection angle, a_y is the missile acceleration and M_α , M_δ , M_q , Z_α and Z_δ are the aerodynamics coefficients. Regarding to Fig.1, the closed-loop transfer function of the three-loop autopilot is written as

$$G_{cl}(s) = \frac{\bar{K}_1(1+T_1s+T_2s^2)}{s^3 + (2\zeta_{AF}\omega_{AF} + \bar{K}_3T_\alpha + \bar{K}_2K_\alpha B_1 + \bar{K}_1T_2)s^2 + \dots + (\omega_{AF}^2 + \bar{K}_3 + \bar{K}_2T_\alpha + \bar{K}_1T_1)s + \bar{K}_1} \quad (2)$$

where

$$\bar{K}_1 = VK_1K_{q3}\omega_{AF}^2, \quad \bar{K}_2 = K_2K_{q3}\omega_{AF}^2, \quad \bar{K}_3 = K_3K_{q3}\omega_{AF}^2 \quad (3)$$

The characteristic polynomial of the closed-loop system with zero steady state error can be described by three positive parameters τ , ζ and ω . These parameters forming a real and a pair of conjugate complex stable poles. The desired close-loop transfer function could be written as

$$G_{cl}(s) = \frac{\tau^{-1}\omega^2(1+T_1s+T_2s^2)}{(s+\tau^{-1})(s^2+2\zeta\omega s+\omega^2)} \quad (4)$$

The positive selection of τ , ζ and ω ensures the closed-loop stability. Moreover, the values of these parameters reflect the performance behavior of the system.

In the following, an analytical formula between the autopilot gains and the design parameters τ , ζ and ω is derived by equating both transfer functions (2) and (4) to obtain

$$\begin{aligned} \bar{K}_3T_\alpha + \bar{K}_2K_\alpha B_1 + \bar{K}_1T_2 &= 2\zeta\omega + \tau^{-1} - 2\zeta_{AF}\omega_{AF} \\ \bar{K}_3 + \bar{K}_2T_\alpha + \bar{K}_1T_1 &= 2\tau^{-1}\zeta\omega + \omega^2 - \omega_{AF}^2 \\ \bar{K}_1 &= \tau^{-1}\omega^2 \end{aligned} \quad (5)$$

$$\begin{pmatrix} \bar{K}_1 \\ \bar{K}_2 \\ \bar{K}_3 \end{pmatrix} = \begin{pmatrix} T_2 & K_\alpha B_1 & T_\alpha \\ T_1 & K_\alpha & 1 \\ 1 & 0 & 0 \end{pmatrix}^{-1} \begin{pmatrix} 2\zeta\omega + \tau^{-1} - 2\zeta_{AF}\omega_{AF} \\ 2\tau^{-1}\zeta\omega + \omega^2 - \omega_{AF}^2 \\ \tau^{-1}\omega^2 \end{pmatrix} \quad (6)$$

$$K = T^{-1}W$$

where the inverse of matrix T is defined for applicable missile parameters with the assumption that $B_1 \ll T_\alpha$. Specifically, each particular gain vector K corresponds to particular combination of the positive values of the design parameters in W through the transformation matrix T. For optimal gain design, the design parameters τ , ζ and ω are tuned to the optimum of certain cost function. The tuning technique should be carried out under the system limitations, these limitations will be highlighted in next section as design constraints.

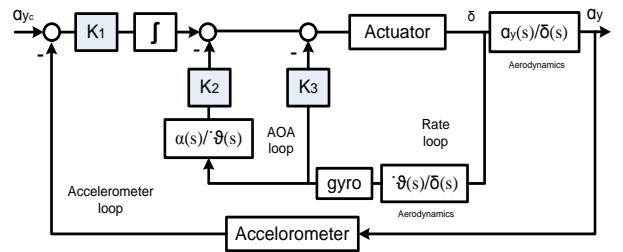


Figure 1. Pseudo AOA autopilot three-loop autopilot.

III. AUTOPILOT DESIGN

The optimal control design could be defined as the control signals that will cause a process to satisfy the physical constraints and at the same time minimize (or maximize) some performance criterion [13]. Precisely, the main objective of the autopilot system is to force the missile to track the steering commands developed by the guidance system. Consequently, the design objective is to

minimize the tracking error between the reference input and the achieved output. However, a free minimization of tracking error may cause too high autopilot gain with unpractical system performance. Here comes the role of the frequency-domain specifications and system limitations in order to quantify the robustness level of the flight control system. One essential parameter that could specify this level is the open-loop crossover frequency. Besides, the physical limit on the actuating system should be considered to avoid the saturation problem. In the following, both the objective and the constraints are manipulated in terms of the design parameters τ , ζ and ω .

A. Design Objective

The ISE between the reference input and the controlled plant output is a powerful quantitative index to measure the tracking performance. The ISE index is expressed as

$$J_{ISE} = \int_0^{\infty} (a_{yc}(t) - a_y(t))^2 dt \quad (7)$$

The ISE is chosen as the command tracking performance index of the autopilot with the consideration of obtaining its analytical expression [14]. Referring to (3), with partial fraction expansion, the unit step response is expressed as

$$a_y(s) = \frac{1}{s} + \frac{c_1}{s + p_1} + \frac{c_2}{s + p_2} + \frac{c_3}{s + p_3} \quad (8)$$

where

$$p_1 = \tau^{-1}, p_2 = \zeta\omega + j\omega\sqrt{1-\zeta^2}, p_3 = \zeta\omega - j\omega\sqrt{1-\zeta^2}$$

$$c_1 = \frac{-\omega^2(\tau^2 - T_1\tau + T_2)}{1 - 2\zeta\tau\omega + \tau^2\omega^2}, c_2 = -M - jN, c_3 = c_2^*$$

$$M = \frac{1 - 2\zeta\tau\omega + T_1\tau\omega^2 - T_2\omega^2}{2(1 - 2\zeta\tau\omega + \tau^2\omega^2)}$$

$$N = \frac{\zeta - 2\zeta^2\tau\omega + \tau\omega + T_1\omega(\zeta\tau\omega - 1) - T_2\omega^2(\tau\omega - \zeta)}{2\sqrt{1-\zeta^2}(1 - 2\zeta\tau\omega + \tau^2\omega^2)}$$

By inverse Laplace transform, the error to the unit step command is expressed as

$$e(t) = 1 - a_y(t) = -c_1 e^{-pt} - c_2 e^{-p_2 t} - c_3 e^{-p_3 t} \quad (9)$$

Therefore the analytical expression of the ISE performance index can be written as

$$J_{ISE}(\tau, \zeta, \omega) = \int_0^{\infty} e^2(t) dt \quad (10)$$

$$= \frac{c_1^2}{2p_1} + \frac{c_2^2}{2p_2} + \frac{c_3^2}{2p_3} + \frac{2c_1c_2}{p_1 + p_2} + \frac{2c_1c_3}{p_1 + p_3} + \frac{2c_2c_3}{p_2 + p_3}$$

The value of the ISE index is always a real positive number due to complex conjugated relation in (9).

B. Autopilot Performance Constraints

The speed of autopilot response should be limited with the required level of robustness consistent with other design constraints such as actuator limits. The system

robustness is described by the open-loop frequency response specifically the crossover frequency.

1) Open-loop crossover frequency constraint

The frequency-domain specifications are specified by the stability margins of the open-loop system. However, ignoring the value of the open-loop crossover frequency in the autopilot design causes system instability for relatively innocuous plant perturbations, even with good phase and gain margins. In fact, such autopilot system has large crossover frequency which indicates that it is attempting to control the high frequency dynamics. As a result, the crossover frequency is an important parameter in the design process to achieve good tradeoff between fastness and robustness. The crossover frequency must be limited to certain chosen value; this value should be high enough to ensure a wide autopilot bandwidth but low enough to prevent stability problems due to actuator, rate gyro and other un-modeled dynamics. References [1,4] introduce a classical “rule of thumb”, which is the crossover frequency should be less than one-third of the actuator bandwidth ω_{ACT} . In order to set a constraint on the open-loop crossover frequency, first, the open-loop transfer function of the three-loop autopilot with loop broken right before the fin actuator is expressed as

$$G_{op}(s) = K_3 G_s^{\beta}(s) + K_2 G_s^{\alpha}(s) + s^{-1} K_1 G_s^{\omega}(s) \quad (11)$$

$$= \frac{(\bar{K}_3 T_{\alpha} + \bar{K}_2 K_{\alpha} B_1 + \bar{K}_1 T_2) s^2 + \dots}{s(s^2 + 2\zeta_{AF} \omega_{AF} s + \omega_{AF}^2)}$$

The open loop magnitude ratio is written as

$$|G_{op}(j\omega_s)|^2 = \frac{(\bar{K}_1 - (\bar{K}_3 T_{\alpha} + \bar{K}_2 K_{\alpha} B_1 + \bar{K}_1 T_2) \omega_s^2)^2 + \dots}{(\omega_{AF}^2 - \omega_s^2)^2 \omega_s^2 + 4\zeta_{AF}^2 \omega_{AF}^2 \omega_s^4} \quad (12)$$

The crossover frequency of practical autopilot is beyond the airframe fundamental dynamic frequency, i.e. $\omega_{AF} < \omega_{CR}$. The crossover frequency magnitude ratio is equal to one, i.e. $|G_{op}(j\omega_{CR})|^2 = 1$. Therefore, the crossover frequency constraint should satisfy the following inequality

$$\left. \frac{(\bar{K}_1 - (\bar{K}_3 T_{\alpha} + \bar{K}_2 K_{\alpha} B_1 + \bar{K}_1 T_2) \omega_s^2)^2 + \dots}{(\omega_{AF}^2 - \omega_s^2)^2 \omega_s^2 + 4\zeta_{AF}^2 \omega_{AF}^2 \omega_s^4} \right|_{\omega_s = \omega_{CRd}} < 1 \quad (13)$$

where ω_{CRd} is the prescribed limitation of ω_{CR} , that is for any gain combination \bar{K}_1 , \bar{K}_2 and \bar{K}_3 satisfying (13) then the corresponding crossover frequency will be $\omega_{CR} \leq \omega_{CRd} < 1/3 \omega_{ACT}$. Regarding to (4) and (12), the crossover frequency constraint function is equivalently expressed in terms of τ , ζ , ω and ω_{CRd} as

$$g(\tau, \zeta, \omega) = (Q_1 - Q_2 \omega_{CRd}^2)^2 + Q_3^2 \omega_{CRd}^2 - C < 0 \quad (14)$$

where

$$Q_1 = \tau^{-1} \omega^2, Q_2 = 2\zeta \omega + \tau^{-1} - 2\zeta_{AF} \omega_{AF}, Q_3 = 2\tau^{-1} \zeta \omega + \omega^2 - \omega_{AF}^2$$

$$C = (\omega_{AF}^2 - \omega_{CRd}^2)^2 \omega_{CRd}^2 + 4\zeta_{AF}^2 \omega_{AF}^2 \omega_{CRd}^4$$

2) Demanded fin-deflection rate constraint

The actuator is a nonlinear device due to its hardware capabilities and limits on fin-deflection and fin-deflection rate. The fin-deflection limit is a physical limit on the moment that the control input can impart on the airframe, which in turn limits the maximum AOA and the normal acceleration. The limit of the fin-deflection rate limits effectively how fast the actuator can cause the missile to rotate, which equally limits how fast the flight control system can respond to changes in the guidance command. Generally, the actuator saturation problem can be safely ignored, if the performance of the autopilot not commands the actuator to exceed its limits. Consequently, the performance of the designed autopilot should be constrained referring to the physical limits of the actuating system. First, the transfer function between input demand acceleration and autopilot command, using the chain rule, is given by

$$\frac{\delta(s)}{a_{yc}(s)} = \frac{\delta(s)}{a_y(s)} * \frac{a_y(s)}{a_{yc}(s)} \quad (15)$$

Referring to (1) and (2), the transfer function is written as

$$G_{a_{yc}}^{\delta}(s) = \frac{\left(\frac{\bar{K}_1}{VK_{q3}} \right) \left(1 + \frac{2\zeta_{AF}s}{\omega_{AF}} + \frac{s^2}{\omega_{AF}^2} \right)}{s^3 + (2\zeta_{AF}\omega_{AF} + \bar{K}_3 T_{\alpha} + \bar{K}_2 K_{\alpha} B_1 + \bar{K}_1 T_2) s^2 + \dots} \quad (16)$$

$$\left(\omega_{AF}^2 + \bar{K}_3 + \bar{K}_2 T_{\alpha} + \bar{K}_1 T_1 \right) s + \bar{K}_1$$

Replacing the nominator terms using (4), the transfer function between input demand acceleration and autopilot command is manipulated in terms of the design parameters as

$$G_{a_{yc}}^{\delta}(s) = \frac{\tau^{-1} \omega^2 \left(\frac{1}{VK_{q3}} \right) \left(1 + \frac{2\zeta_{AF}s}{\omega_{AF}} + \frac{s^2}{\omega_{AF}^2} \right)}{s^3 + (2\zeta \omega + \tau^{-1}) s^2 + (2\tau^{-1} \zeta \omega + \omega^2) s + \tau^{-1} \omega^2} \quad (17)$$

The steady-state gain of the previous transfer function is totally determined by the aerodynamic parameters and the flight velocity of the missile, which are considered to be designed such that the demanded steady-state fin-deflection is within the missile actuating limit all over the flight operating condition. Normally, the maximum value of the demanded fin-deflection rate corresponding to commanded acceleration is achieved as the frequency of its transfer function tends to infinity; this value should be limited referring to the physical limit of the actuator fin-deflection rate. Moreover, setting limit on the maximum value of the autopilot command rate is also limits the transient performance of the fin-deflection. Similarly, such limit could efficiently govern the system non-minimum phase response [15].

$$\left| G_{a_{yc}}^{\delta}(s) \right|_{\max} = \lim_{s \rightarrow \infty} s G_{a_{yc}}^{\delta}(s) = \frac{\tau^{-1} \omega^2}{VK_{q3} \omega_{AF}^2} \quad (18)$$

Commonly, the practical actuating system is described by the maximum fin-deflection rate $\dot{\delta}_{\lim}$ with the corresponding maximum fin-deflection rate demand $\dot{\delta}_{\max}$ at each operating point, so the demanded acceleration command is limited by

$$\sup |a_{yc}(s)| \leq \left(\frac{VK_{q3} \omega_{AF}^2}{\tau^{-1} \omega^2} \right) \dot{\delta}_{\max}$$

where $\dot{\delta}_{\max} = \gamma \dot{\delta}_{\lim}$ and ($\gamma \geq 1$) is a scalar factor based on the actuator hardware dynamics. In the same meaning, the autopilot design perimeters τ and ω are limited by specified actuator fin-angle rate $\dot{\delta}_{\lim}$ and maximum acceleration command $a_{yc\max}$ as

$$\tau^{-1} \omega^2 \leq VK_{q3} \omega_{AF}^2 \left(\frac{\gamma \dot{\delta}_{\lim}}{a_{yc\max}} \right)$$

The inequality constraint of rate actuating limit is given as

$$\Delta(\tau, \omega) = \tau^{-1} \omega^2 - VK_{q3} \omega_{AF}^2 \left(\frac{\gamma \dot{\delta}_{\lim}}{a_{yc\max}} \right) < 0 \quad (19)$$

C. Inequality Constrained Optimization

The optimal autopilot design problem can be stated in the form of inequality constrained optimization problem as

$$\begin{aligned} \min_{\tau, \zeta, \omega} & : J_{ISE}(\tau, \zeta, \omega) \\ \text{Subject_to} & : g(\tau, \zeta, \omega) < 0, \Delta(\tau, \omega) < 0 \\ \text{Bounds} & : \tau > 0, \omega > 0, \zeta_{\min} < \zeta < 1 \end{aligned} \quad (20)$$

where $\zeta_{\min} > 0$ is the lower limit of the autopilot closed loop damping factor. This limit is, about 0.7, considered to guarantee a sufficient level of system damping and phase margin since the crossover frequency cannot describe the total performance requirements [16]. The optimization problem (20) is the core of the introduced optimal technique, where the objective function is the performance evaluation scale and the constraints are the performance limitations for practical design. The bounds of the design parameters are set to positive values to ensure the system stability for the whole space of the cost function. Moreover, the constraints divide this space into two domains, the feasible domain where the constraints are satisfied, and the infeasible domain where at least one of the constraints is violated. Mostly, the optimum design is found on the boundary between the feasible and infeasible domains, that is at a point where at least one of the constraints equal zero.

The method of Lagrange multipliers is one of advanced optimization techniques which applied to such constrained optimization problem [16]. The method of Lagrange relies on maximizing or minimizing an associated function called the augmented Lagrangian

function. The augmented function is constructed by combined the objective function with the constraint equations through a set of non-negative real parameters called Lagrange multipliers $\lambda_j \geq 0$. The augmented Lagrangian function of the optimization problem Eq. (20) is written as

$$J(\tau, \zeta, \omega, \lambda_1, \lambda_2) = J_{ISE}(\tau, \zeta, \omega) + \lambda_1 g(\tau, \zeta, \omega) + \lambda_2 \Delta(\tau, \omega) \quad (21)$$

More compactly, let $x = (\tau, \zeta, \omega)$ and $\lambda = (\lambda_1, \lambda_2)$. The necessary conditions for local optimal solution are given by Karush Kuhn-Tucker (KKT) conditions as

$$\begin{aligned} \nabla J(\hat{x}, \hat{\lambda}) &= \frac{\partial J(x)}{\partial x} + \lambda_1 \frac{\partial g(x)}{\partial x} + \lambda_2 \frac{\partial \Delta(x)}{\partial x} = 0 \\ g(\hat{x}) &\leq 0 \\ \Delta(\hat{x}) &\leq 0 \end{aligned} \quad (22)$$

where ∇ denoted the first-order derivative and $(\hat{x}, \hat{\lambda})$ refers to the optimal solution. The KKT conditions are necessary but not sufficient for optimality. However, if the optimization problem is convex, then the KKT conditions are sufficient for global optimality [16]. A sufficient condition for optimality is that the Hessian matrix of the Lagrangian function, the second derivative, is positive definite. The Hessian matrix of the Lagrangian function is given as

$$H = \nabla^2 f(x) + \lambda_1 \nabla^2 g(x) + \lambda_2 \nabla^2 \Delta(x) \quad (23)$$

Particularly, this problem is a nonlinear constrained multi-variable optimization problem. As expected, the function **fmincon** of the MATLAB Optimization Toolbox can solve such kind of smooth objective optimization problem well effectively with feasible initial design parameters. Moreover, it converges to the same minimum point even starting from different initial guesses. In this line of thought, the optimal autopilot gains K_1 , K_2 and K_3 are easily calculated by substituting the optimum parameters $\hat{\tau}$, $\hat{\zeta}$ and $\hat{\omega}$ into (6) and (3) without need for design weight's adjustment.

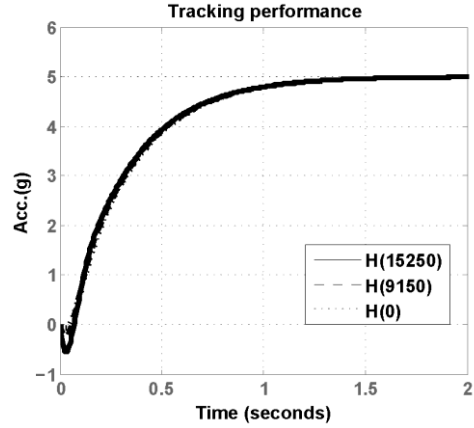
IV. NUMIRICAL ANALYSIS

In this section, numerical analysis is carried out to show the effectiveness of the proposed optimal technique for the autopilot design. Data of a typical missile system at different operating points [17], listed in the Table 1, are used to for this purpose. Moreover, the actuator is considered as a second-order dynamic system with natural frequency $\omega_{ACT} = 220 \text{ rad s}^{-1}$, damping factor $\zeta_{ACT} = 0.65$, maximum fin deflection rate $\dot{\delta}_{im} = 300 \text{ deg s}^{-1}$ and maximum fin deflection $\pm 10 \text{ deg}$. Let the limit of the open-loop crossover frequency is equal to $\omega_{Crd} = 50 \text{ rad s}^{-1}$, less than one third of actuator dynamic. The numerical data in Table 1 are for three operating points at different attitudes with same speed

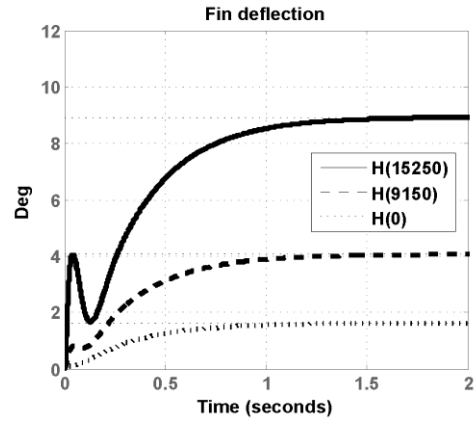
$V = 914 \text{ m s}^{-1}$ and maximum demand acceleration of $a_{yc_{max}} = 5g$.

TABLE I. TYPICAL MISSILE AERODYNAMIC DATA

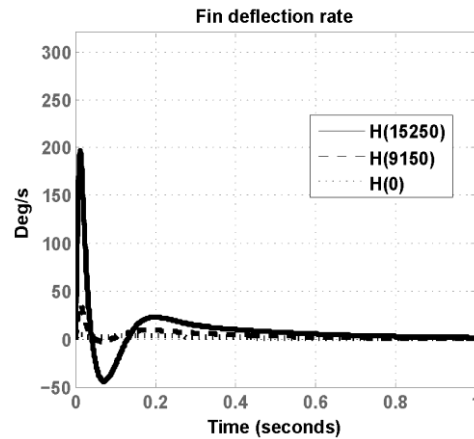
P	H (m)	ω_{AF} (rad/s)	M_α (s^{-2})	M_δ (s^{-2})	Z_α (s^{-1})	Z_δ (s^{-1})
1	0	25.43	642	555	2.94	0.65
2	9150	15.49	240	204	1.17	0.239
3	15250	9.95	99.1	81.7	0.533	0.0957



(a) Response of 5g acceleration



(b) Fin-deflection response



(c) Fin-deflection rate response

Figure 2. Performance of desired crossover frequency strategy.

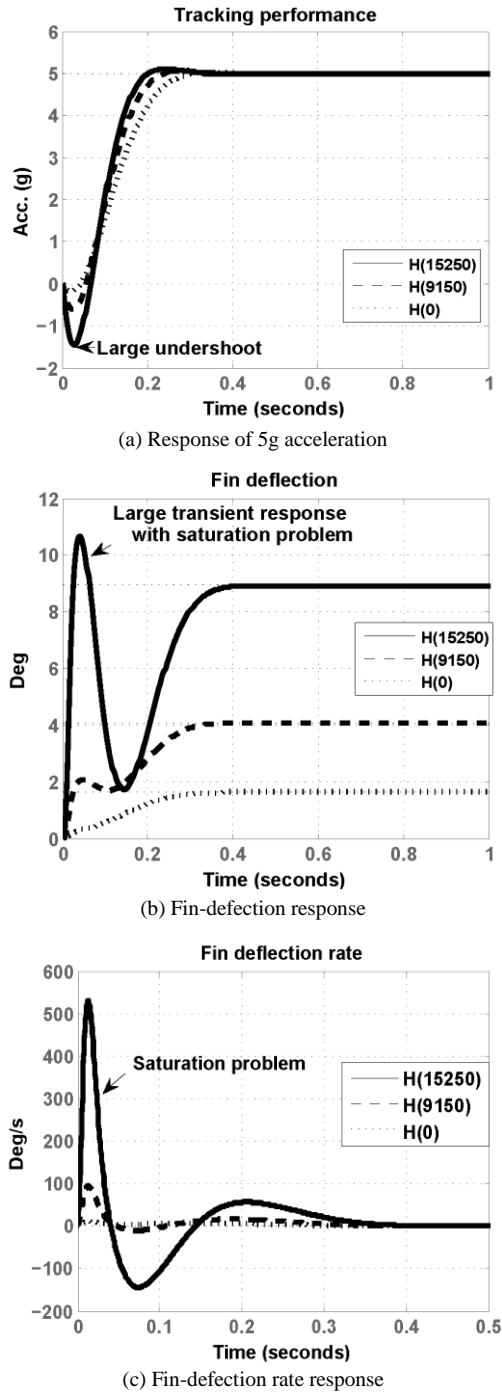


Figure 3. Performance of proposed technique with single-constraint

The autopilot performances for these three points using the design strategy in Ref. [17] are shown in Fig. 2. This strategy is considered as a pole adjustment technique where the desired pole position is described similarly by the desired characteristic parameters. Both τ and ζ are pre-defined by the designer while ω is tuned to minimize the crossover frequency objective of minimum $|\omega_{CR} - \omega_{CRd}|$ without a clear formula. Besides, this strategy limits the autopilot performance to certain specified level by fixing the values of the design parameters τ and ζ despite this system could achieves better tracking within applicable design parameters.

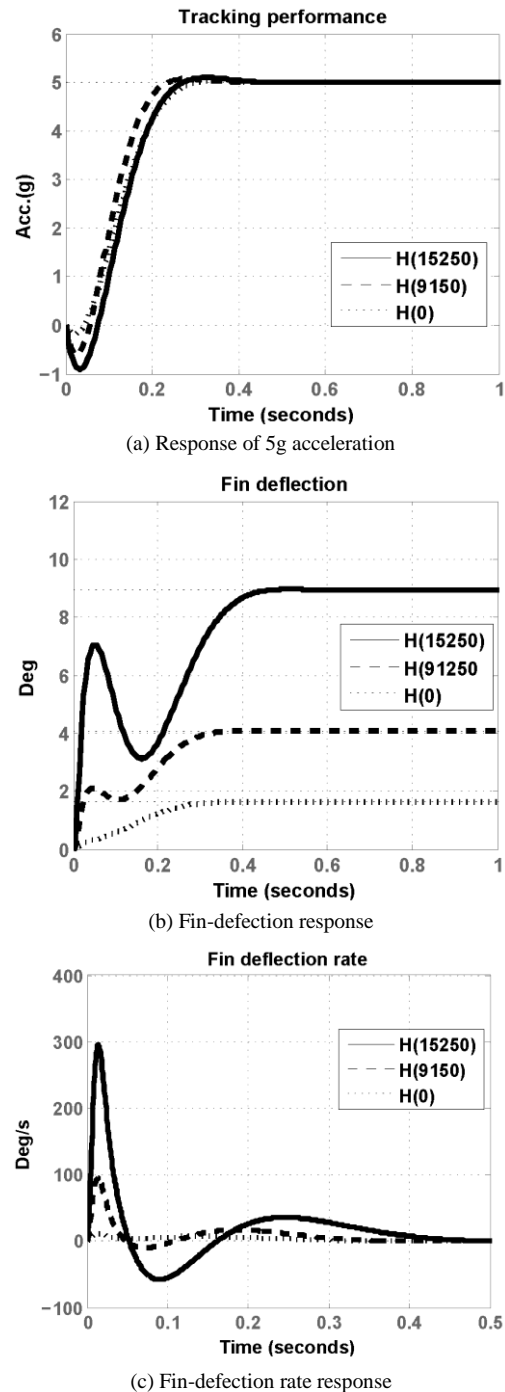


Figure 4. Performance of proposed technique with Multi-constraint

Moreover, the crossover frequency is an important parameter for practical design but it cannot totally describe the system performance requirements, so it is better neither considered as a performance objective of the autopilot design-schemes nor neglected. In the following, the proposed technique is applied to provide the optimal autopilot design at these operating points. Here, the optimization problem Eq. (20) is solved to minimize the objective function (10) within the validation of the constraint functions Eq. (14) and Eq. (19). In order to emphasize the importance of the two constraints, the design will be handled for two cases.

TABLE II. DESIGN PERFORMANCE COMPARISON.

H (m)	Desired ω_{CR} Strategy			Single-constraint design			Multi-constraint design		
	0	9150	15250	0	9150	15250	0	9150	15250
τ	0.3	0.3	0.3	0.0651	0.058	0.065	0.0651	0.058	0.074
ζ	0.7	0.7	0.7	0.7	0.7	0.7	0.7	0.7	0.7
ω	26.8	29.6	30.3	19.34	21.4	23.4	19.34	21.4	17.8
K_1	0.002	0.0176	0.093	0.005	0.047	0.268	0.005	0.047	0.138
K_2	-0.207	-3.58	-11.5	-0.1	-3.34	-11.2	-0.1	-3.34	-6.6
K_3	0.071	0.237	0.672	0.077	0.28	0.881	0.077	0.28	0.622
ω_{CR} rad s ⁻¹	49.92	49.96	50.01	50.03	50.02	50.01	50.03	50.02	40.4
PM °	88.3	71.4	67	89.97	72.6	67.4	89.97	72.6	69.5

First, the single-constraint case, the crossover frequency constraint is only considered. The optimal design performance of the three-loop autopilot at the three operating points is exhibited in Fig. 3. It is clear in Fig.3 (a) that the design achieves much better tracking performance than the other strategy in Fig. 2 (a) with almost same crossover frequency and phase margin as shown in Table 2. Moreover, the related fin deflections and fin deflection rates are demonstrated in Fig. 3 (b) and (c) where the elevator deflections of the three operating points reach to the same steady values as in Fig. 2 (b) since these values are totally determined by the aerodynamic parameters and the flight velocity of the missile. Besides, the slight larger elevator deflections and deflection rates introduced by the proposed technique during transient time is served as a payment for the faster response. However, at the height $H=15250$, the proposed technique with single-constraint shows some degradations as the large non-minimum phase response and saturation problems for fin deflection and fin deflection rate. These problems are addressed by applying the multi-constraint design.

Second, the multi-constraint case is applied where both the crossover frequency and the actuator demanded rate limits are considered. As illustrate in Fig. 4 and listed in the Table 2 the system performances for the operating conditions $H=9150$ and $H=0$ achieve the same tracking and frequency performances as in case of single-constraint. The reason is that the condition for fin deflection rate is not violated through these two operating points. On the other hand, at the point $H=15250$ the single-constraint optimal design achieves the crossover frequency within the design limit but with fin deflection rate greater than the applicable limit. Meanwhile, using the multi-constraint, the fin-deflection rate constraint is activated to achieve the optimum design within both constraints.

V. CONCLUSION

The three-loop autopilot is considered for optimal gain design using multi-constraint optimization technique. The tracking performance is established analytically as the design objective. Moreover, the design practicality and robustness are achieved by inequality constraints on the system open-loop crossover frequency and the maximum

demand of fin-deflection rate. The optimal solution is provided by constrained optimization. The whole design is manipulated in terms of stable characteristic parameters of the autopilot closed-loop, and in such way that the tradeoff between tracking performance and robustness is brought directly into the design process without need for weights to adjust. Numerical simulations show the importance of the demanded fin-deflection rate constraint for practical design since the crossover frequency cannot describe the total performance requirements. Moreover, the proposed method provides a better tracking performance with the required robustness level compared with another design strategy.

REFERENCES

- [1] F. W. Nesline and P. Zarchan, "Why modern controllers can go unstable in practice," *Journal of Guidance, Control, and Dynamics* vol. 7, no. 4, pp. 495-500, Jul. 1984.
- [2] S. Talole, A. Godbole, J. Kolhe, and S. Phadke, "Robust roll autopilot design for tactical missiles," *Journal of Guidance, Control, and Dynamics*, vol. 34, no. 1, pp. 107-117, Jan. 2011.
- [3] P. B. Jackson, "Overview of missile flight control systems," *Johns Hopkins APL Technical Digest*, vol. 29, no. 1, pp. 9-24, Jan. 2010.
- [4] P. Zarchan, *Tactical and strategic missile guidance*, 4 th ed. American Institute of Aeronautics and Astronautics, Reston VA, 2002, ch. 24, pp. 507-520.
- [5] V. S. Chellaboina, W. M. Haddad, and J. H. Oh, "Fixed-order dynamic compensation for linear systems with actuator amplitude and rate saturation constraints," *International Journal of Control*, vol. 73, no. 12, pp. 1087-1103, 2000.
- [6] C. Hai-rong and Z. Yue, "Three-loop autopilot design and simulation," in *Proc. International Conf. on Mechatronics and Automation (ICMA)*, Chengdu, IEEE, 2012, pp. 2499-2503.
- [7] F. Jun-fang, S. Zhong, L. Qing, and D. Si-yu, "Design and control limitation analysis of two-loop autopilot," in *Proc. Control and Decision Conference (CCDC)*, China, IEEE, 2011, pp. 3814-3818.
- [8] L. Defu, F. Junfang, Q. Zaikang, and M. Yu, "Analysis and improvement of missile three-loop autopilots," *Journal of Systems Engineering and Electronics*, vol. 20, no. 4, pp. 844-851, Aug. 2009.
- [9] X. Lidan, Z. Ke'nan, C. Wanchun, and Y. Xingliang, "Optimal control and output feedback considerations for missile with blended aero-fin and lateral impulsive thrust," *Chinese Journal of Aeronautics*, vol. 23, no. 4, pp. 401-408, Aug. 2010.
- [10] Y. Li, K. Zheng, and X. Chen, "Rapidly limitation analysis of three-loop acceleration autopilot," *Journal of Projectiles, Rockets, Missiles and Guidance*, vol. 33, no. 3, pp. 17-24, June 2013.
- [11] M. A. Duarte-Mermoud and R. A. Prieto, "Performance index for quality response of dynamical systems," *ISA Transactions*, vol. 43, no. 1, pp. 133-151, Jan. 2004.
- [12] M. J. Patra, P. S. Khuntia, and M. S. Samal, "Analysis and comparison of different performance index factor for conventional

PID & GA plus PID controller,” *International Journal of Emerging Technologies in Computational and Applied Sciences*, vol. 4, no. 3, pp. 242-250, May. 2013.

- [13] D. E. Kirk, *Optimal Control Theory: an Introduction*, Courier Corporation, 2012, ch. 1, pp. 3-17.
- [14] M. Abd-elatif, L. Qian, and Y. Bo, “Optimization of three-loop missile autopilot gain under crossover frequency constraint,” *Defence Technology*, vol. 12, no. 1, Feb. 2015.
- [15] C. P. Mracek and D. B. Ridgely, “Missile longitudinal autopilots: connections between optimal control and classical topologies,” in *Proc. AIAA Guidance, Navigation and Control Conference and Exhibit*, San Francisco, California, Aug. 2005, pp. 1-29.
- [16] D. P. Bertsekas, *Constrained Optimization and Lagrange Multiplier Methods*, 1 st ed., Academic press, USA, 2014, ch. 3, pp. 231-260.
- [17] W. Qiu-Qiu, X. Qun-Li, and Q. Zai-kang, “Pole placement design with open-loop crossover frequency constraint for three-loop autopilot,” *Journal Systems Engineering and Electronics*, vol. 2, pp. 420-423, 2009.



Qian Longjun was born in China, received his BSc and MSC degree in Mathematics from Northeastern Normal University in 1986 and 1989, his PhD degree in Control Theory and Control Engineering from Northeastern University in 1997. He is now a Professor of Control Theory and Control Engineering in the School of Automation at Nanjing University of Science and Technology, Nanjing, China. His research interests include flight control and stochastic control. He has published more than 20 papers in refereed journals.



Mohamed Abd-Elatif was born in Egypt, 1976. He is a research engineer in MRC (Egypt). Currently, He is a doctoral student in the School of Automation, Nanjing University of Science and Technology. His research interests include flying vehicle control, guidance, overall design and hardware implementation.